IMPROVED LOGARITHMIC WAVEFORM INVERSION CONSIDERING THE POWER-SPECTRUM OF THE WAVEFIELD

YOUNGSEO KIM[1], YOUNG HO CHA[1], CHANGSOO SHIN[1], SEUNGWON KO[2] and YOUNGTAK SEO[2]

[1] *Department of Energy Resources Engineering, Seoul National University, 599 Gwanak-ro, Gwanak-gu, Seoul 151-742, South Korea.*
[2] *Korea National Oil Corporation, Gwanyang-dong, Dongan-gu, Anyang-si, Gyeonggi-do 431-711, South Korea.*

(Received April 21, 2008; revised version accepted February 9, 2009)

ABSTRACT

Kim, Y.S, Cha, Y.H., Shin, C.S., Ko, S.W. and Seo, Y.T., 2009. Improved logarithmic waveform inversion considering the power-spectrum of the wavefield. *Journal of Seismic Exploration*, 18: 215-228.

Local minima of an objective function in waveform inversion often prevent solutions from converging to the global minimum in cases where an initial velocity model for the inversion is far from the true velocity structure. In particular, forward-modeled wavefields with small power-spectrum values in the logarithmic objective function cause the numerical instability in the calculation of the gradient direction. Hence, it is important to remove these small values to allow a solution of the logarithmic objective function to converge to the global minimum. To mitigate the instability, we developed a frequency-domain waveform inversion algorithm taking into consideration the power-spectrum of the wavefield in the process of the calculation of the logarithmic objective function. By calculating the objective function using only wavefields with relatively large values of the power-spectrum, we confirmed that the number of local minima was reduced and the shape of the misfit function was suitable for the gradient-type inversion. We demonstrated our technique for waveform inversion through two numerical examples of the 2D profiles of SEG/EAGE salt and overthrust models.

KEYWORDS: waveform inversion, frequency domain, logarithmic objective function, power spectrum, filtering technique.

0963-0651/09/$5.00

INTRODUCTION

Studies on seismic imaging and inversion comprise two different categories: direct and indirect methods (Amundsen et al., 2006). The direct inversion method is closely related to seismic imaging concepts used to find earth material properties (Claerbout, 1971; Keys and Weglein, 1983; Weglein et al., 2003). The indirect inversion method usually seeks a desired solution by minimizing the objective function (Pratt et al., 1998; Shin and Min, 2006). In this study, we focus on the frequency-domain waveform inversion that minimizes the logarithmic objective function, which is a misfit between the observed and forward-modeled data, among indirect inversion methods. However, the waveform inversion has some pitfalls: (1) an inadequate model type may be used to invert for an inappropriate/unrealistic set of parameters, (2) low frequency missing may cause difficulty in producing reasonable results, and (3) searching for local minima may lead to useless and misleading results. Lailly (1983) and Tarantola (1984) introduced the back-propagation algorithm for time-domain seismic inversions and their ideas contributed to improvements in waveform inversion methods. The back-propagation algorithm could help to reduce the computational cost of calculating a gradient direction because we do not need to compute the partial derivative wavefields directly. Many studies have been conducted on frequency-domain waveform inversions based on their ideas, and the back-propagation algorithm could be applied to frequency-domain waveform inversion (Pratt et al., 1998).

Frequency-domain waveform inversion has several advantages over time-domain waveform inversion: (1) computational efficiency through multiple source simulation, (2) easy source estimation, and (3) feasible application for parallel computation. As mentioned above, waveform inversion minimizes the objective function to find a desired solution. Thus, the appropriate selection of the objective function is very important in waveform inversion. Shin and Min (2006) introduced a frequency-domain waveform inversion using the logarithmic wavefield for an objective function, which yielded a more competitive seismic inversion method than conventional methods. However, waveform inversion using the logarithmic wavefield still needs to overcome the local minima problem and requires the estimation of a good initial model that is close to the true model.

Wavefields with small power-spectrum values affect inversion results only slightly in the conventional frequency-domain waveform inversion method. However, the objective function of logarithmic waveform inversion is very sensitive to these small values, which cause numerical instability in calculating the gradient direction. In this study, we proposed a technique to filter out the wavefields with small power-spectrum values in calculating the gradient direction. By using this technique, the stability in the calculation of the gradient

direction and local minima problem in the waveform inversion were improved. We demonstrated our waveform inversion algorithm for 2D profiles of the SEG/EAGE salt and Overthrust models (Aminzadeh et al., 1997).

GRADIENT DIRECTION OF THE LOGARITHMIC OBJECTIVE FUNCTION

The basic concept of waveform inversion is to update model parameters until a convergence criterion for an objective function to be minimized is satisfied. The objective function using a logarithmic wavefield for 2D acoustic frequency-domain waveform inversion (Shin and Min, 2006) can be written as:

$$E(\mathbf{m}) = \tfrac{1}{2} \sum_{i}^{N_f} \sum_{j}^{N_s} \sum_{k}^{N_r} (\ln u_{ijk} - \ln d_{ijk})(\ln u_{ijk} - \ln d_{ijk})^* \quad . \tag{1}$$

In eq. (1), $\mathbf{m}$ is the subsurface velocity vector; u_{ijk} and d_{ijk} are the forward-modeled and measured wavefields in the frequency domain, respectively, for the k-th receiver, the j-th source, and the i-th frequency; * indicates the complex conjugate; and N_f , N_s and N_r are the numbers of frequencies, sources, and receivers, respectively. The gradient direction of the logarithmic objective function for a frequency, which is the steepest-descent direction (Shin et al., 2007), can be derived as:

$$\partial E/\partial m_l = \mathrm{Re}[(\mathbf{v}_l)^{\mathrm{T}} \mathbf{S}^{-1} \mathbf{r}] \quad ,$$

$$\mathbf{v}_l = -(\partial \mathbf{S}/\partial m_l)\mathbf{u} \quad ,$$

$$\mathbf{r} = \left[\frac{1}{u_{ij1}} \left(\ln \frac{u_{ij1}}{d_{ij1}} \right)^* \quad \frac{1}{u_{ij2}} \left(\ln \frac{u_{ij2}}{d_{ij2}} \right)^* \quad \cdots \quad \frac{1}{u_{ijN_r}} \left(\ln \frac{u_{ijN_r}}{d_{ijN_r}} \right)^* \quad 0 \quad \cdots \quad 0 \right]^T \quad . \tag{2}$$

$$(i = 1, 2, \cdots, N_f,\ j = 1, 2, \cdots, N_s,\ l = 1, 2, \cdots, N_p)$$

In eq. (2), $\mathbf{S}$ is the complex impedance matrix of the finite element method (FEM) for the 2D frequency-domain wave equation, $\mathbf{v}$ is the virtual source, $\mathbf{r}$ is the residual vector, N_p is the total number of model parameters, m_l is the l-th element of subsurface velocity vector $\mathbf{m}$, and $\mathbf{u}$ is the forward-modeled wavefield in the frequency domain. Because of the reciprocal of the forward-modeled wavefield in the residual vector, wavefields with small power-spectrum values can cause numerical instability in calculating the gradient direction. Therefore, we proposed a filtering technique to remove wavefields with small power-spectrum values in the calculation of the gradient direction.

FILTERING TECHNIQUE FOR THE LOGARITHMIC OBJECTIVE FUNCTION

Since the logarithmic objective function of waveform inversion for seismic data usually has many local minima, it is difficult for a solution to converge to the global minimum unless an initial model is close to the true velocity structure. To investigate the effect of our modified logarithmic objective function in which the modeled wavefields which have small values for the power-spectrum are removed, we calculated the original logarithmic (Shin and Min, 2006) and modified objective functions for a simplified velocity model from the 2D A-A′ profile of the SEG/EAGE salt model. The test model was generated by two parameters, consisting of the velocity of a salt dome and the gradient of the linearly increasing background velocity. To calculate the objective functions, we assume that Fig. 1a is the true velocity model, where the velocity of the salt dome is 4.5 km/s and the velocity of the background increases linearly with depth from 1.5 km/s to 3.5 km/s. Fig. 1b is an example of the estimated model used to calculate the objective function.

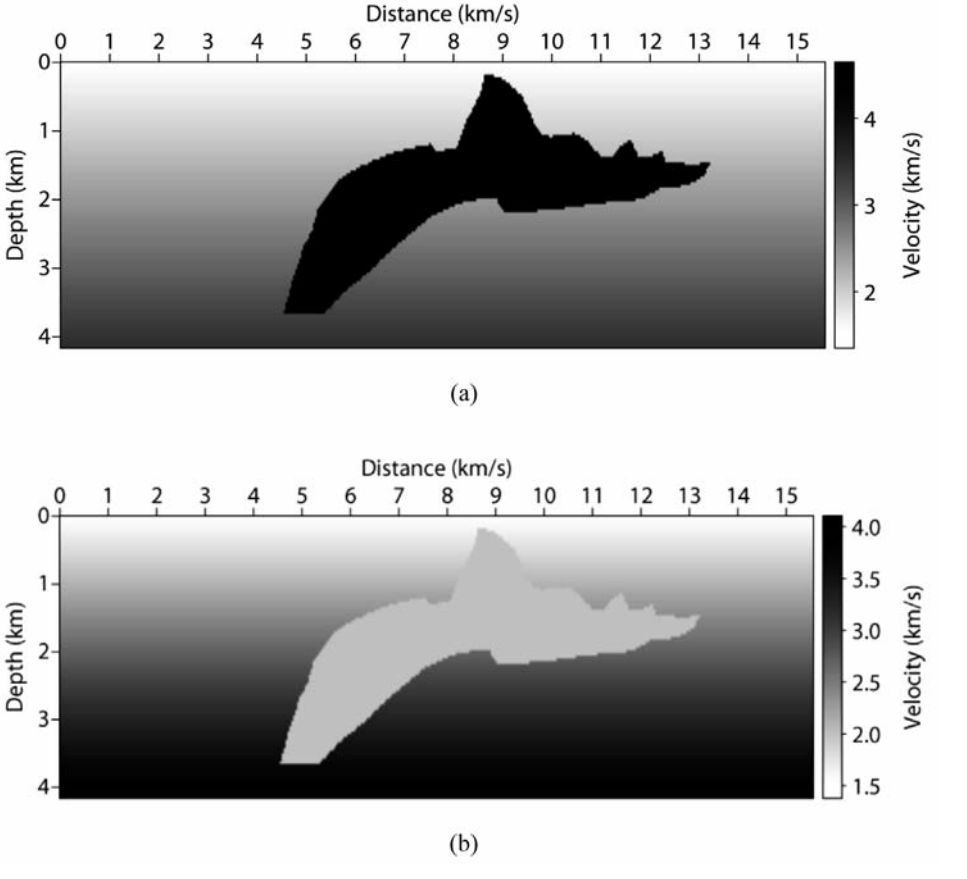

Fig. 1. Simplified SEG/EAGE salt models: (a) salt velocity: 4.5 km/s; background velocity: 1.5-3.5 km/s, (b) salt velocity: 2 km/s; background velocity: 1.5-3.98 km/s.

Contour maps of the objective function at three frequencies, 0.8, 1.2, and 14.4 Hz, with respect to the changes in both the velocity of the salt dome and the gradient of background velocity are shown in Fig. 2. The vertical and horizontal axes represent the velocity of the salt dome (V_S) and the maximum value of the background velocity (V_{max}), respectively. Fig. 2 shows that the original logarithmic objective function of waveform inversion has a number of local minima even for this simplified model. Therefore, if an initial velocity model for inversion is not chosen near the global minimum (V_S = 4.5 km/s, V_{max} = 3.5 km/s), the solution of the inversion cannot converge to the global minimum by the steepest-descent method. We note that it is more difficult to find the global minimum point for the velocity of the salt dome at higher frequencies (Fig. 2c).

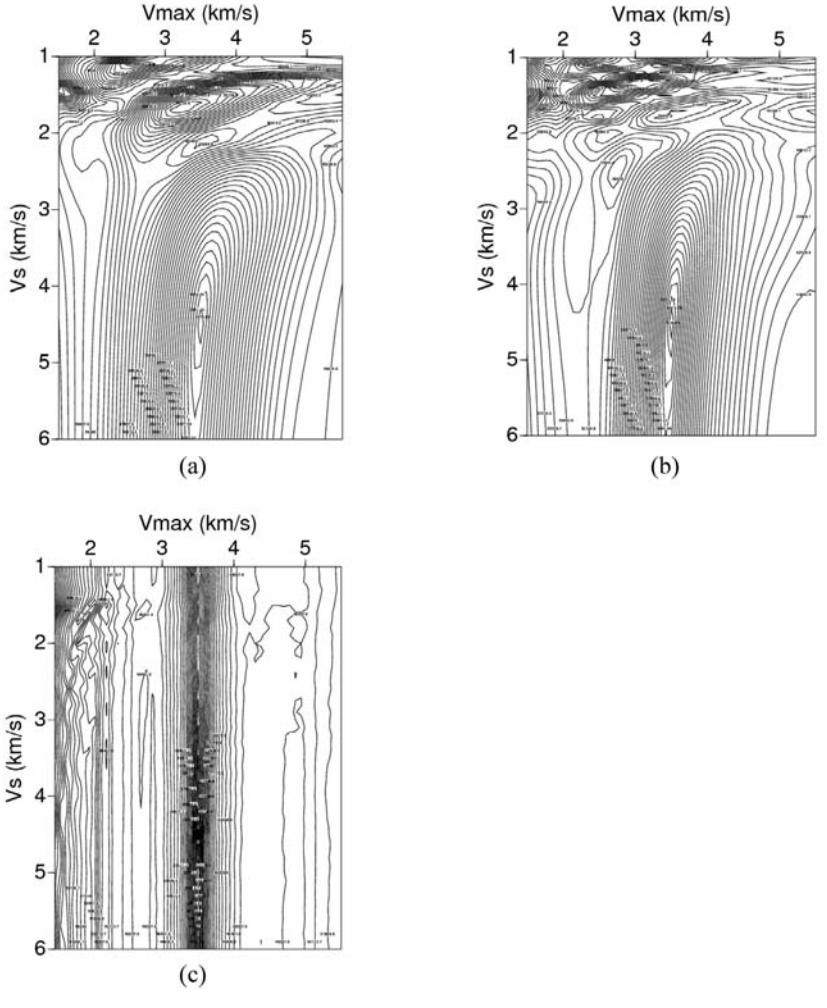

Fig. 2. Contour maps of the logarithmic objective function in the frequency domain at frequencies of (a) 0.8 Hz, (b) 1.2 Hz, (c) 14.4 Hz.

As we mentioned in the previous section, the logarithmic objective function is very sensitive to wavefields with small power-spectrum values. Accordingly, we hypothesized that filtering out these small values might mitigate the instability of the logarithmic objective function. To show the effect of filtering out small values, contour maps of the objective function using wavefields with the largest 10% of the power-spectrum values are shown in Fig. 3, where sources, receivers, and frequencies are the same as those used in Fig. 2. We note that many of the local minima are removed by this filtering technique. In particular, local minima completely disappear in the case of the frequency of 0.8 Hz (Fig. 3a). These results indicate that we might obtain the

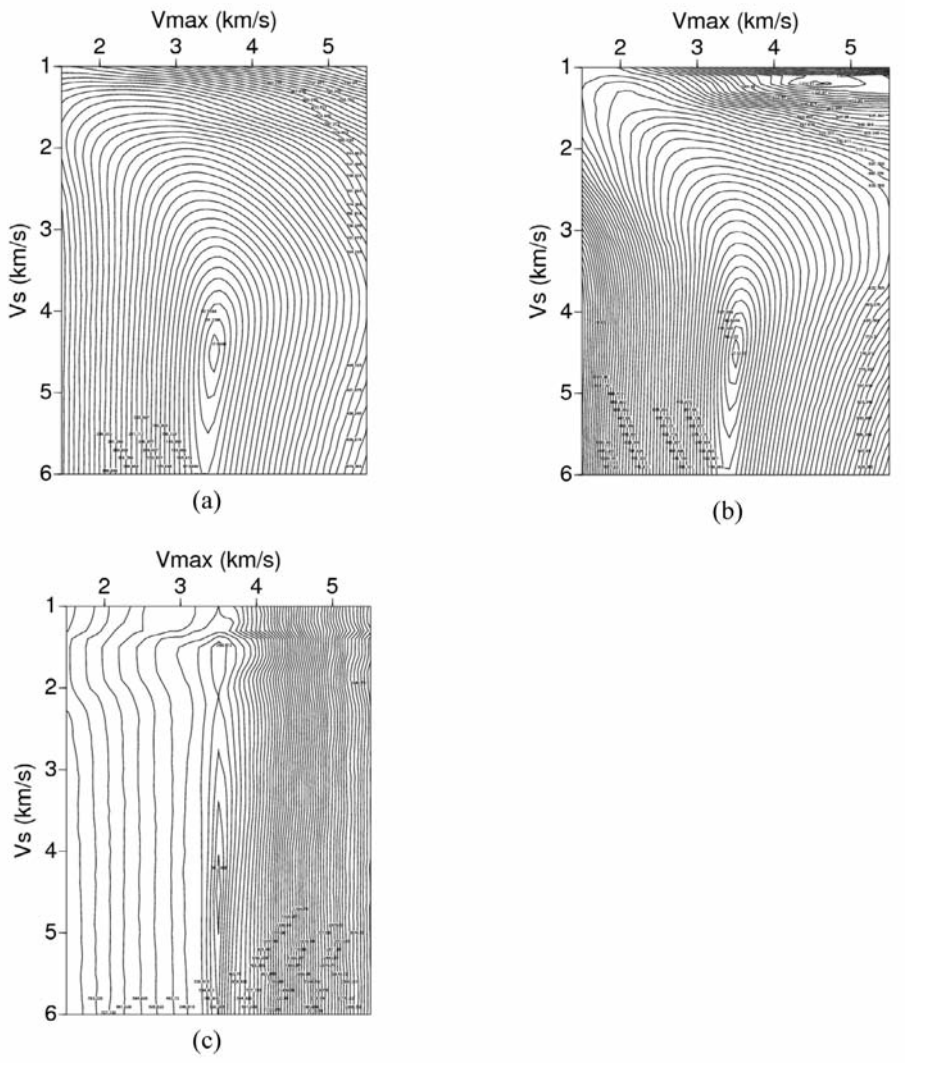

Fig. 3. Contour maps of the logarithmic objective function generated by the largest 10% of the data in the frequency domain at frequencies of (a) 0.8 Hz, (b) 1.2 Hz, (c) 14.4 Hz.

desired inverted velocity structure (V_S = 4.5 km/s, V_{max} = 3.5 km/s) with this filtering technique even if the waveform inversion were performed using a linearly increasing model as an initial model. In the case of the high frequency of 14.4 Hz, a solution of the inversion can converge to the global minimum using the gradient-type inversion method (Fig. 3c).

If the wavefields of the small power-spectrum are the components comprising the significant event, it might be meaningless to exclude them in the process of the calculation of the gradient direction in the waveform inversion.

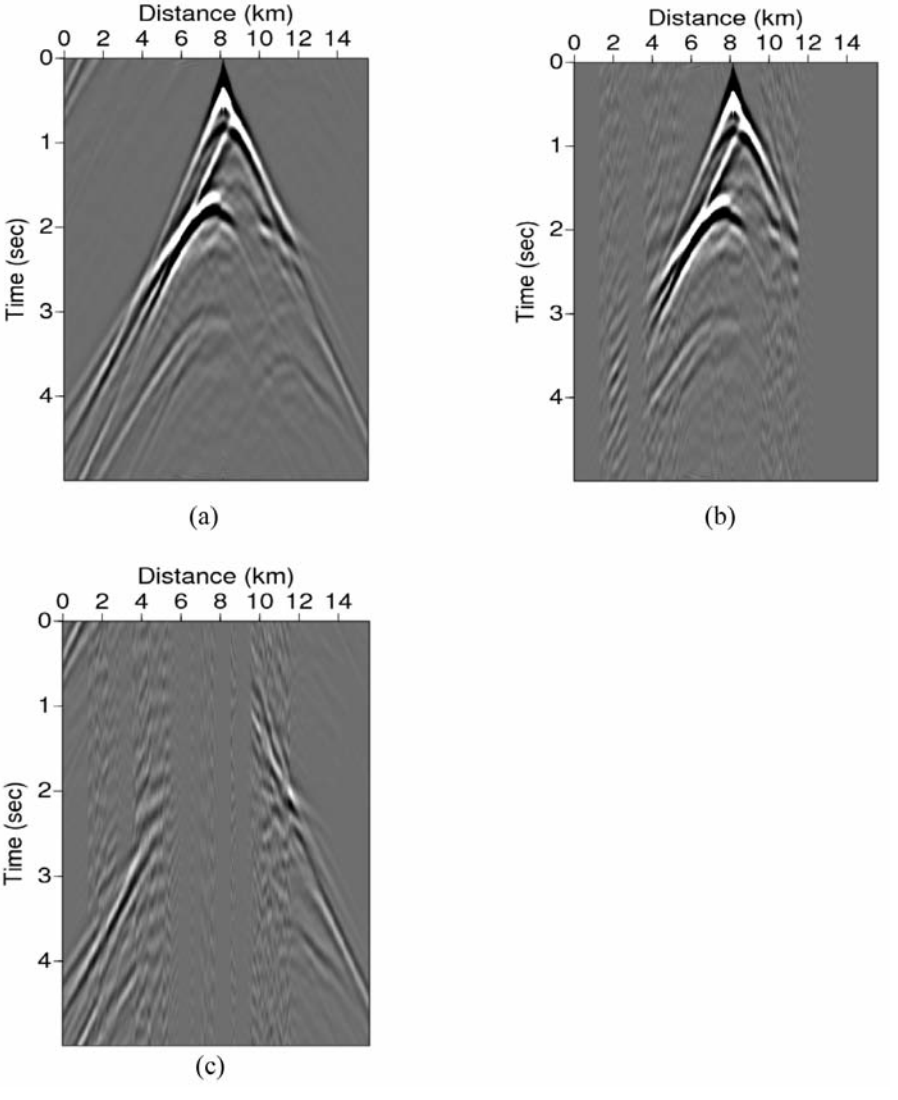

Fig. 4. Seismograms for the salt model shown in Fig. 5a, (a) original seismogram, (b) seismogram constructed using the largest 40% of values from the original seismogram, (c) seismogram constructed using the smallest 60% of values from the original seismogram.

To validate the filtering technique, we generated time-domain synthetic seismograms for the salt model in Fig. 5a using only the small or large values of the power-spectrum. Fig. 4a displays the original time-domain synthetic seismogram, Fig. 4b is generated by the largest 40% of the power-spectrum values, and Fig. 4c is generated by the smallest 60% of the values. We note that wavefields with small power-spectrum values are mostly related to late arrivals and far offset traces (Fig. 4c). However, the time-domain seismogram generated by large power-spectrum values in Fig. 4b contains the strong direct waves and reflections. These results show that the filtering technique for the logarithmic objective function tries to use only strong signals or early time signals in the original data. Thus, this technique using wavefields with relatively large values of the power-spectrum might help the waveform inversion to converge to the global minimum. Two numerical examples using this technique are demonstrated in the next section.

NUMERICAL EXAMPLES

The 2D A-A′ profile of the SEG/EAGE salt model

To verify our filtering-out technique for the logarithmic objective function, we performed the waveform inversion for the 2D A-A′ profile of the SEG/EAGE salt model. To generate the observed data for inversion, we used 2D acoustic frequency-domain FEM modeling for the velocity model in Fig. 5a. We used the first derivative Gaussian function with a central frequency of 3.8 Hz for the source wavelet and performed the logarithmic waveform inversion for 38 frequencies ranging from 0.2 to 7.4 Hz. The grid size was 40 m, and 381 shots and 381 receivers at 40 m intervals were used. A velocity model that increases linearly with depth from 1.5 km/s to 3.5 km/s was used as an initial model (Fig. 5b). The source wavelet was also inverted using the full Newton method simultaneously (Shin and Min, 2006). When the logarithmic waveform inversion was performed without the filtering technique, a solution of the inversion did not converge to the global minimum. Only the velocity structures near the surface were well recovered, but the salt body and sub-salt regions were not accurately inverted (Fig. 5c).

We then performed the waveform inversion using wavefields of the largest 10% of the power-spectrum values (Fig. 6). Because the filtering technique can enhance the shape of the logarithmic objective function, we were able to obtain an inverted velocity structure that was very similar to the true model. Although the sub-salt regions were not well recovered, the upper and lower boundaries of the salt body, the velocity of the salt dome, the background velocity model, and the artificial layers were accurately recovered.

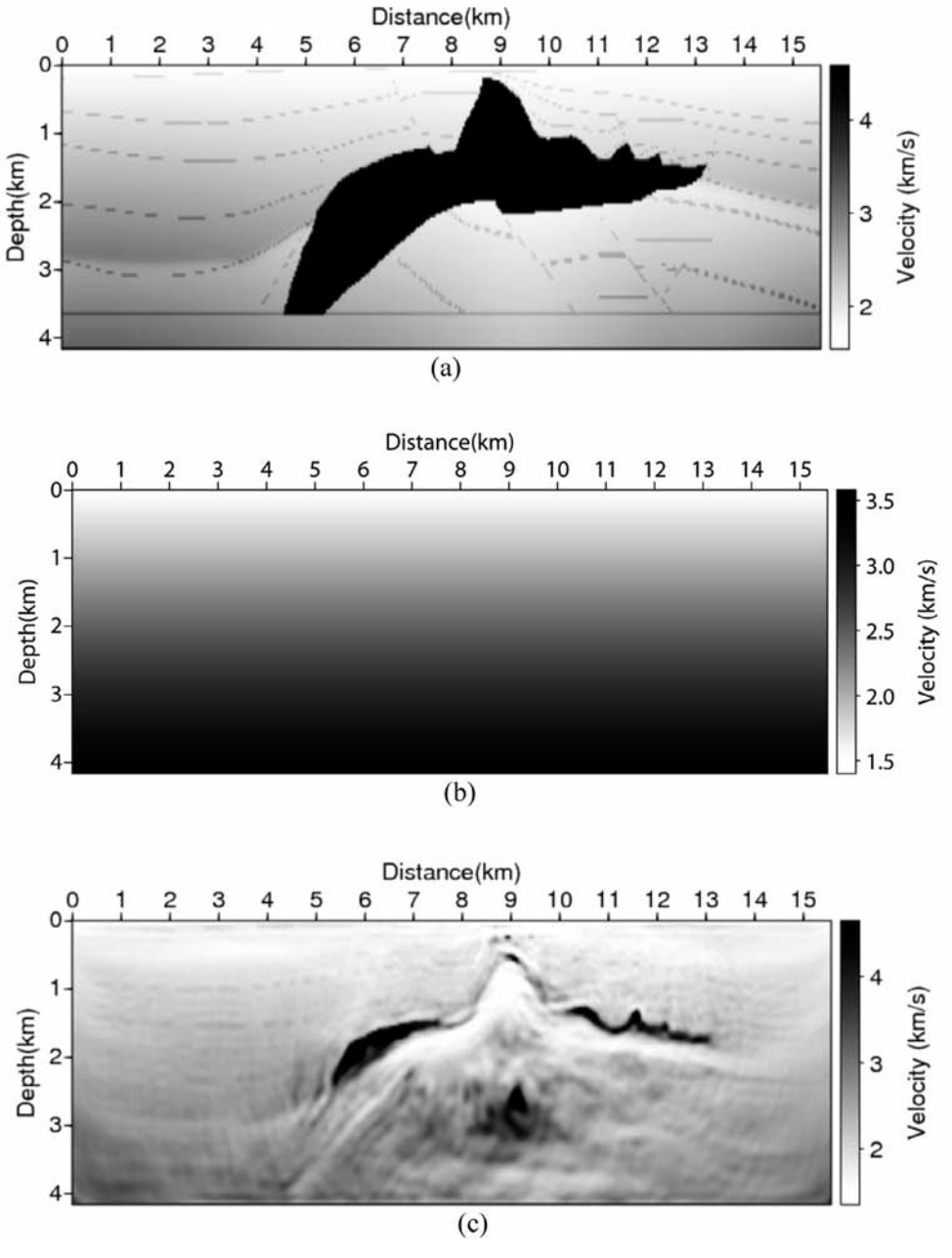

Fig. 5. (a) The 2D A-A′ profile of the SEG/EAGE salt model, (b) an initial velocity model, (c) the inverted velocity model at the 400-th iteration using the logarithmic waveform inversion without the filtering technique.

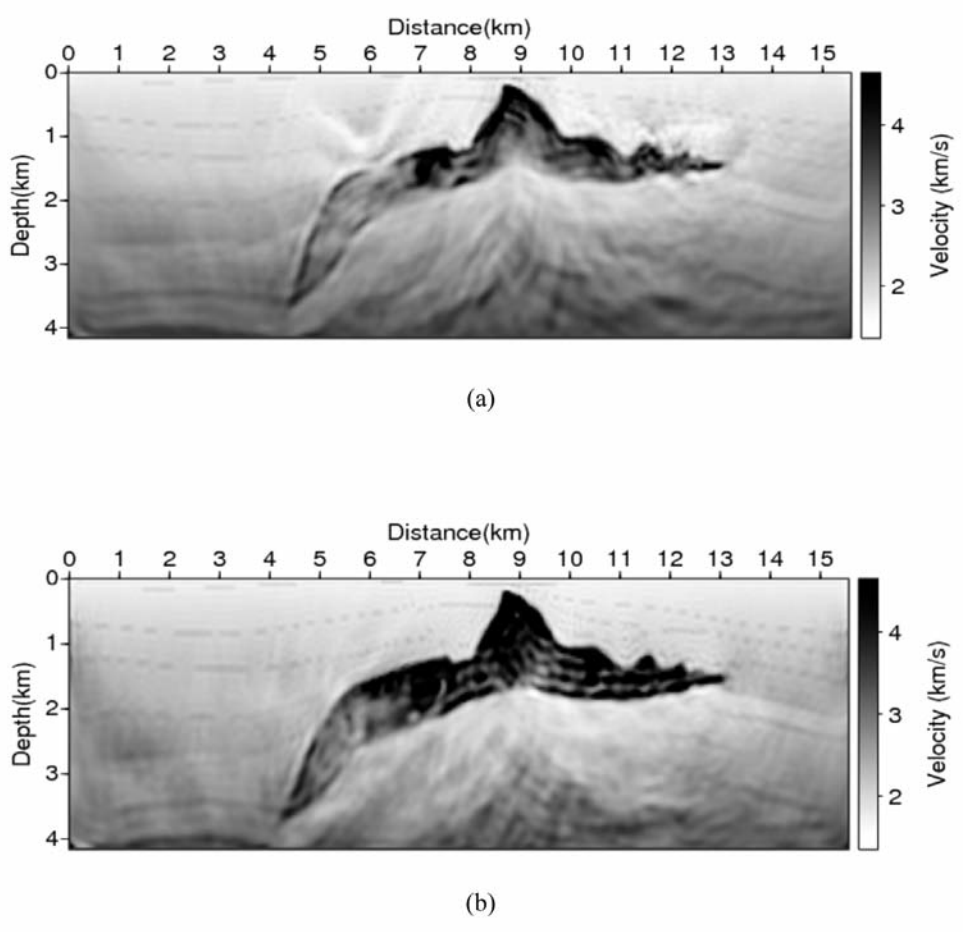

Fig. 6. The inverted velocity model of the logarithmic wavefields using the largest 10% of the forward modeled wavefields at the (a) 400-th and (b) 950-th iterations.

The Overthrust model

For the second example, we conducted the waveform inversion for the Overthrust model (Fig. 7a). The first derivative Gaussian source with a central frequency of 7.6 Hz was also used as the source wavelet. We performed the waveform inversion for 76 frequencies ranging from 0.2 to 15 Hz. A velocity model that increased linearly with depth from 3 km/s to 6 km/s was used as an initial model (Fig. 7b). The grid size was 25 m, and 398 shots and 398 receivers at 50 m intervals were used. When the logarithmic waveform inversion

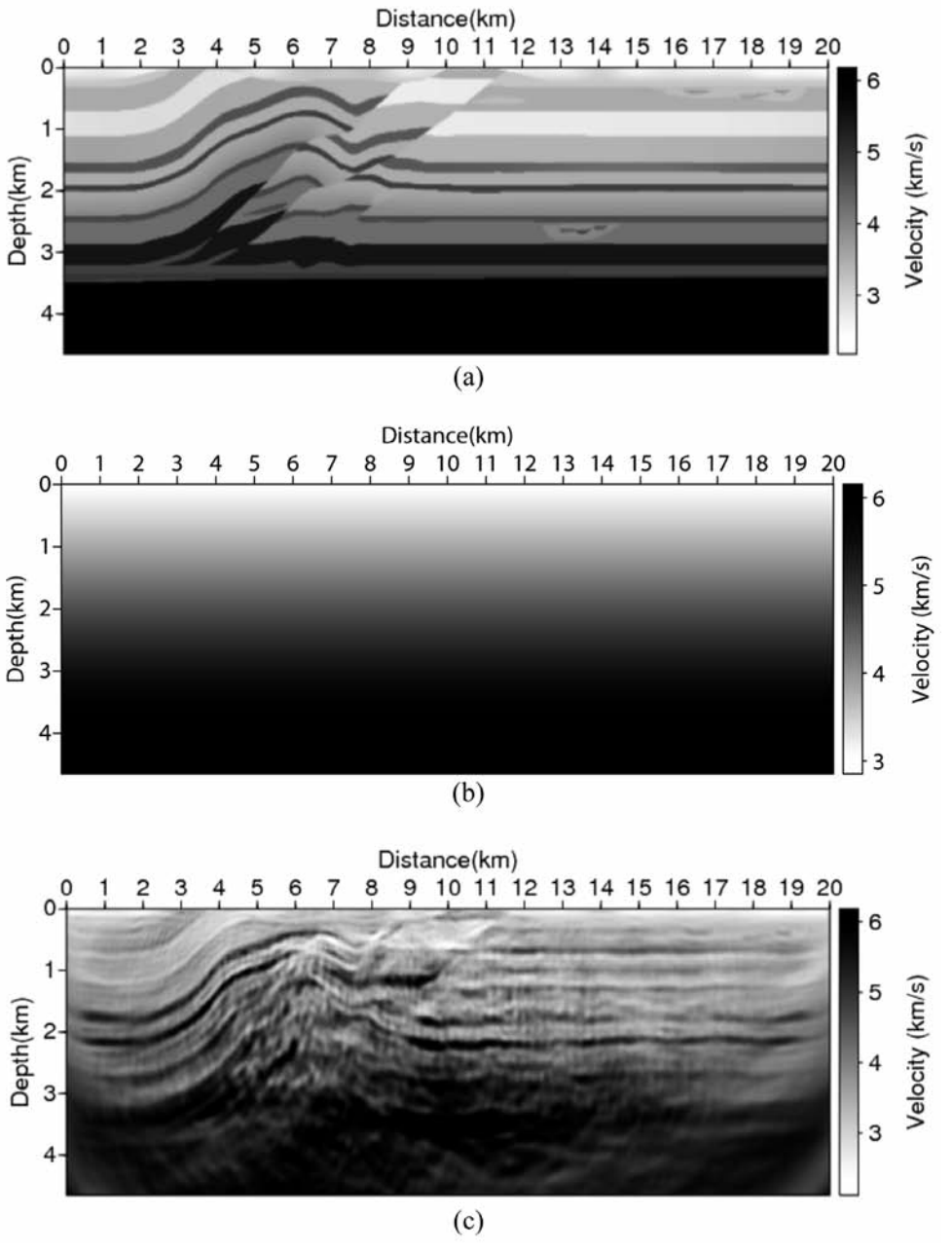

Fig. 7. (a) The SEG/EAGE Overthrust model, (b) an initial velocity model, (c) the inverted velocity model at the 150-th iteration using waveform inversion without the filtering technique.

without filtering was conducted for this model, the shallow parts near the two faults and overthrust were quite distorted, and the deeper part of the model was not inverted accurately (Fig. 7c). When we performed the waveform inversion for this model using wavefields with the largest 10% of the power-spectrum values, the inverted velocity model contained the significant features of the true model (Fig. 8a). However, because 90% of the wavefields were excluded by the filtering technique, some critical information for the inversion might be removed as well. Thus, the slightly fluctuating layers in the inverted velocity model in Fig. 8a might be caused by the lack of information.

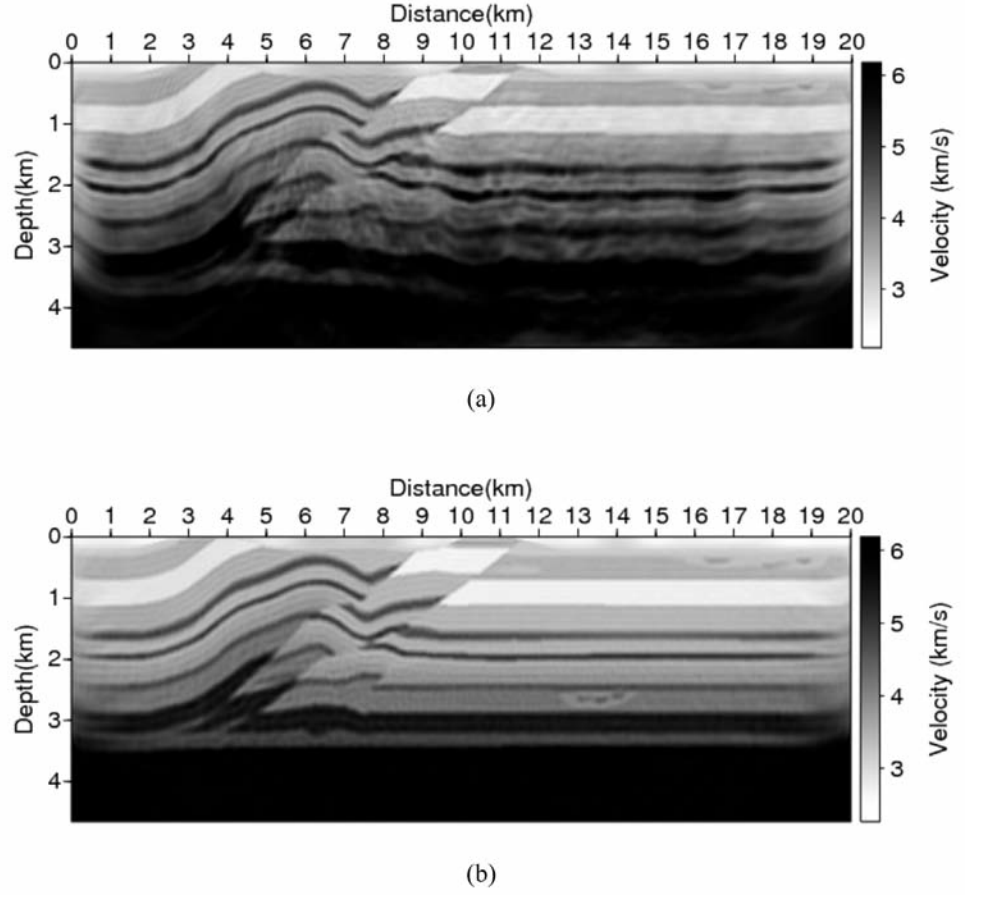

Fig. 8. (a) The inverted velocity model at the 150-th iteration using logarithmic wavefields using the largest 10% of the forward modeled wavefields, (b) the inverted velocity model at the 300-th iteration using all the data, where the inverted velocity model of Panel (a) was used as the initial velocity model.

We noted that the inversion using only wavefields with large power-spectrum values was able to provide the inverted velocity model near the global minimum. Thus, we re-performed the inversion using all the data without the filtering, where the inverted velocity model in Fig. 8a generated using the filtering technique was used as the initial model. Since the initial velocity model was very close to the true model, the logarithmic waveform was able to provide the inverted velocity model (Fig. 8b), which was almost the same as the true one (Fig. 7a).

CONCLUSIONS

The objective function for logarithmic waveform inversion is very sensitive to wavefields with small power-spectrum values. By generating a time-domain synthetic seismogram using only small and large values of the power-spectrum, we found that the wavefields with small power-spectrum values are closely related to far offset traces or late arrivals and they might make it difficult to find a solution using the logarithmic objective function that converges to the global minimum.

The number of local minima was largely reduced by excluding the wavefields of these small power-spectrum values in the calculation of the logarithmic objective function for a simplified velocity model. Two numerical examples using the filtering technique were demonstrated and we were able to obtain reasonable results that were close to the true model. Although an initial model was not close to the true velocity structure, the filtering technique was able to improve the convergence of the waveform inversion to the global minimum. This meant that the stability of the gradient direction in the logarithmic waveform inversion was improved when these small values were excluded from the calculation of the logarithmic objective function. Finally, when the inverted velocity model with the filtering technique was used as an initial model for the waveform inversion using all data, a more enhanced and converged inversion result, which was almost the same as the true model, was obtained. Further studies will be required to determine the optimal percentage of wavefields for the logarithmic waveform inversion.

ACKNOWLEDGEMENTS

This work was supported by the Korea Science and Engineering Foundation (KOSEF) grant funded by the Korean government (MOST) (No. R0A-2006-000-10291-0), the Brain Korea 21 project of the Ministry of Education and Korea National Oil Corporation grant (velocity modeling using full waveform inversion), and the Energy Technology Innovation (ETI) project funded by the Ministry of Knowledge Economy, Korea.

REFERENCES

Aminzadeh, F., Brac, J. and Kunz, T., 1997. 3-D Salt and Overthrust Models. SEG, Tulsa, OK.

Amundsen, L., Reitan, A., Arntsen, B. and Ursin, B., 2006. Acoustic nonlinear amplitude versus angle inversion and data-driven depth imaging in stratified media derived from inverse scattering approximations. Inverse Problems, 22: 1921-1945.

Claerbout, J.F., 1971. Toward a unified theory of reflector mapping. Geophysics, 36: 467-481.

Keys, R.G. and Weglein, A.B., 1983. Generalized linear inversion and the first Born theory for acoustic media. J. Math. Phys., 24: 1444-1449.

Lailly, P., 1983. The seismic inverse problem as a sequence of before stack migration. In: Bednar, J.B., Rednar, R., Robinson, E. and Weglein. A.B. (Eds.), Conference on Inverse Scattering: Theory and Application. Soc. Industr. Appl. Mathemat., Philadelphia: 208-220.

Pratt, R.G., Shin, C. and Hicks, G.J., 1998. Gauss-Newton and full Newton methods in frequency domain seismic waveform inversion. Geophys. J. Internat., 133: 341-362.

Shin, C. and Min, D.J., 2006. Waveform inversion using a logarithmic wavefield. Geophysics, 71: R31-R42.

Tarantola, A., 1984. Inversion of seismic reflection data in the acoustic approximation. Geophysics, 49: 1259-1266.

Weglein, A.B., Araujo, R.V., Carvalho, P.M., Stolt, R.H., Matson, K.H., Coates, R.T., Corrigan, D., Foster, D.J., Shaw, S.A. and Zhang, H., 2003. Inverse scattering series and seismic exploration. Inverse Problems, 19: R27-R83.